



# Isolation, genomic characterization, and pathogenicity of a Chinese porcine deltacoronavirus strain CHN-HN-2014



Nan Dong<sup>a,b</sup>, Liurong Fang<sup>a,b</sup>, Hao Yang<sup>a,b</sup>, Han Liu<sup>a,b</sup>, Ting Du<sup>a</sup>, Puxian Fang<sup>a,b</sup>, Dang Wang<sup>a,b</sup>, Huanchun Chen<sup>a,b</sup>, Shaobo Xiao<sup>a,b,\*</sup>

<sup>a</sup> Key Laboratory of Agricultural Microbiology, College of Veterinary Medicine, Huazhong Agricultural University, Wuhan 430070, China

<sup>b</sup> The Cooperative Innovation Center for Sustainable Pig Production, Wuhan 430070, China

## ARTICLE INFO

### Article history:

Received 14 June 2016

Received in revised form 14 October 2016

Accepted 17 October 2016

### Keywords:

Porcine deltacoronavirus (PDCoV)

Chinese strain

Genome characterization

Pathogenicity

## ABSTRACT

Porcine deltacoronavirus (PDCoV) is an emerging swine coronavirus that causes diarrhea in piglets. Since the first outbreak of PDCoV in the United States in 2014, this novel porcine coronavirus has been detected in South Korea, Canada, Mexico, Thailand, and China. In this study, a Chinese PDCoV strain, designated CHN-HN-2014, was isolated from piglets with severe diarrhea on a pig farm in Henan Province, China, and examined with a specific immunofluorescence assay and electron microscopy. Genomic analysis showed that CHN-HN-2014 shares 91.6%–99.4% nucleotide identity with other known PDCoV strains. The pathogenicity of CHN-HN-2014 was further investigated in 5-day-old and 21-day-old piglets. Both kinds of piglets developed clear clinical symptoms, including vomiting, anorexia, lethargy, and severe diarrhea, by 2 days postinoculation (DPI), and diarrhea persisted for about 5–6 days. Viral shedding was detected in rectal swabs until 14 DPI in challenged 5-day-old pigs and until 18 DPI in challenged 21-day-old pigs. At necropsy at 4 DPI, macroscopic and microscopic lesions were observed and viral antigen was detected in the small intestines with immunohistochemical staining. These data demonstrate that Chinese PDCoV strain CHN-HN-2014 shares high nucleotide identity with previously reported PDCoV strains and is pathogenic in 5-day-old and 21-day-old piglets.

© 2016 Elsevier B.V. All rights reserved.

## 1. Introduction

Porcine deltacoronavirus (PDCoV) is an enveloped, single-stranded, positive-sense RNA virus belonging to the genus *Deltacoronavirus*, in the family *Coronaviridae*. PDCoV was first identified in pig feces in Hong Kong during the molecular surveillance of coronaviruses (CoVs) in avian and mammalian species in 2011 (Woo et al., 2010, 2012). Based on a molecular evolutionary genetic analysis of known CoVs, the CoV ancestor is tentatively divided into a bat CoV lineage and a bird CoV lineage, which evolved into the genera *Alphacoronavirus* and *Betacoronavirus* and the genera *Gammacoronavirus* and *Deltacoronavirus*, respectively (Woo et al., 2012). PDCoV is genetically close to the bird CoV lineage but infects pigs (Woo et al., 2012).

PDCoV was first detected in farmed pig with diarrhea in February 2014 in Ohio, USA (Wang et al., 2014a). To date, it has been

reported in at least 18 states of the United States, Canada, South Korea, China, Mexico, and Thailand (Wang et al., 2014b; Ma et al., 2015; Homwong et al., 2016; Janetanakit et al., 2016; Jung et al., 2016; Lee et al., 2016; Zhang, 2016). A retrospective epidemiological study showed that PDCoV was detected in pig samples as early as August 2013 in the United States (McCluskey et al., 2015) and in pig samples in South Korea in May 2014 (Lee et al., 2015). Some groups have recently reported the emergence of PDCoV in different areas of the Chinese mainland, and interestingly, we detected PDCoV in pig diarrhea samples collected as early as 2004 (Chen et al., 2015a, 2015b; Dong et al., 2015; Song et al., 2015; Wang et al., 2015a, 2015b). With increased concern about this newly emerging enteric disease, reverse-transcription polymerase chain reaction (RT-PCR), real-time RT-PCR, nested RT-PCR, and singleplex RT insulated isothermal PCR methods have been developed to detect PDCoV in clinical samples (Marthaler et al., 2014; Wang et al., 2014a; Song et al., 2015; Zhang et al., 2015, 2016). Enzyme-linked immunosorbent assays for PDCoV-specific serum antibodies, based on the PDCoV S1 or nucleocapsid protein, have also been used to determine the prevalence of anti-PDCoV immunoglobulin G (IgG) in pig serum (Su et al., 2015; Thachil et al., 2015).

\* Corresponding author at: College of Veterinary Medicine, Huazhong Agricultural University, 1 Shi-zi-shan Street, Wuhan 430070, China.  
E-mail address: [vet@mail.hzau.edu.cn](mailto:vet@mail.hzau.edu.cn) (S. Xiao).

It was recently reported that PDCoV strains OH-FD22 and OH-FD100 cause severe atrophic enteritis, accompanied by severe diarrhea and vomiting within 11–14 days in gnotobiotic pigs (Jung et al., 2015). The subsequent isolation and pathogenicity of several cell-culture-adapted PDCoV strains (USA/IL/2014, Michigan/8977/2014), and Ohio CVM I were also confirmed (Chen et al., 2015a, 2015b; Hu et al., 2015; Ma et al., 2015). A histopathological study of naturally PDCoV-infected pigs was consistent with previous pathogenetic studies, and the lesions were similar to but relatively milder than those caused by *Porcine epidemic diarrhea virus* (PEDV), another enteropathogenic porcine coronavirus (Wang et al., 2015a, 2015b).

However, although evidence of the prevalence of PDCoV in China is accumulating, detailed information on PDCoV isolates from China is rarely reported. In this study, we isolated the Chinese PDCoV strain CHN-HN-2014 in LLC-PK1 cells, characterized its complete genome, and investigated its pathogenicity in 5-day-old and 21-day-old pigs with a clinical assessment, the quantification of viral shedding and distribution, histology, and immunohistochemistry.

## 2. Materials and methods

### 2.1. Clinical samples and treatment

Totally 21 PDCoV-positive diarrhea samples (five intestinal contents and 16 feces) were attempted for PDCoV isolation. These samples were collected from commercial pig farms in Hubei, Jiangsu, Anhui, Henan, and Guangdong Provinces in late 2014, and tested with M- and N-gene-based RT-PCRs as previously reported by Wang et al. (2014a). To get the inoculum for virus isolation, 1 ml of PDCoV-positive intestinal contents were homogenized in 10 ml of Dulbecco's modified Eagle's medium (DMEM), and the suspension was centrifuged at  $4200 \times g$  for 10 min at  $4^\circ\text{C}$ . The supernatants were separated and filtered through  $0.22 \mu\text{m}$  filters. As for the feces samples, 1 g of PDCoV-positive feces was suspended in 10 ml of DMEM, vortexed for 5 min, and then centrifuged at  $4200 \times g$  for 10 min at  $4^\circ\text{C}$ . The supernatants were separated and filtered through  $0.22 \mu\text{m}$  filters. The filtered supernatants were used as the inoculum for PDCoV isolation.

### 2.2. Virus isolation, plaque purification, propagation, and titration

PDCoV was isolated in the LLC-PK1 cell line (American Type Culture Collection No. CL-101). The growth medium for LLC-PK1 cells was DMEM containing 10% fetal bovine serum, and the maintenance medium for PDCoV propagation was DMEM supplemented with  $10 \mu\text{g/ml}$  trypsin (Gibco, USA).

When the LLC-PK1 cell monolayers in six-well cell culture plates reached 70%–80% confluence, they were washed three times with maintenance medium. An aliquot ( $500 \mu\text{l}$ ) of filtered sample, together with 1.5 ml of maintenance medium, was added to each well. After viral adsorption for 1 h at  $37^\circ\text{C}$ , the cells were washed three times with maintenance medium, and 2 ml of maintenance medium was added to each well. The cells were then cultured continuously at  $37^\circ\text{C}$  in 5%  $\text{CO}_2$ . When an obvious cytopathic effect (CPE) was observed in 80%–90% of cells 1–2 days after inoculation, the plate was twice frozen at  $-80^\circ\text{C}$  and thawed. The supernatants were stored at  $-80^\circ\text{C}$  as seed stocks for plaque purification and subsequent passage. The isolated PDCoV strain, CHN-HN-2014, was plaque purified as described previously (Hu et al., 2015).

For PDCoV propagation, 70%–80% confluent LLC-PK1 cells in a T25 flask were washed three times with maintenance medium, and then 5 ml of maintenance medium and  $5 \mu\text{l}$  of PDCoV were added. The cells were cultured at  $37^\circ\text{C}$  in 5%  $\text{CO}_2$ . After an obvious CPE was observed at 1–2 days, the infected cells were twice frozen at  $-80^\circ\text{C}$

and thawed, and the supernatants were stored at  $-80^\circ\text{C}$  until subsequent passage.

Viral titers were determined as the 50% tissue culture infectious dose ( $\text{TCID}_{50}$ ) on LLC-PK1 cells in a 96-well plate, as described previously (Hu et al., 2015).

### 2.3. Immunofluorescence assay (IFA)

LLC-PK1 cells in 24-well cell culture plates were mock infected or infected with PDCoV at a multiplicity of infection (MOI) of 0.01. At 24 h after inoculation, the cells were fixed with 4% paraformaldehyde for 15 min and then permeabilized with 0.2% Triton X-100 for 10 min at room temperature. The cells were incubated with a PDCoV-N-protein-specific monoclonal antibody, which was produced from hybridoma cells derived from Sp2/0 myeloma cells and spleen cells of BALB/c mice immunized with recombinant N protein of PDCoV strain CHN-HN-2014, and with a fluorescein-isothiocyanate-labeled goat anti-mouse secondary antibody (Santa Cruz Biotechnology) for 1 h. The cell nuclei were counterstained with 4',6-diamidino-2-phenylindole for 15 min at room temperature. After the cells were washed with phosphate-buffered saline (PBS), the stained cells were observed with a fluorescence microscope (Olympus IX73, Japan).

### 2.4. Electron microscopic observation

LLC-PK1 cells infected with PDCoV were harvested when an obvious CPE was observed. The cells were frozen and thawed three times, and then the cell culture was centrifuged at  $4200 \times g$  at  $4^\circ\text{C}$  for 1 h (Hitachi CR21GIII, Japan). The supernatant was filtered through a  $0.22 \mu\text{m}$  filter to remove the cell debris. The filtered supernatant was then ultracentrifuged at  $30,000 \times g$  for 4 h at  $4^\circ\text{C}$  to pellet the PDCoV particles. The viral particle pellets were resuspended in PBS and then negatively stained with 2% phosphotungstic acid and examined with a transmission electron microscope (Hitachi H-7000FA, Japan).

### 2.5. Complete genomic analysis

Total RNA was extracted from the cell culture samples with the E.Z.N.A. Total RNA Kit I (Omega Bio-tek, USA). Reverse transcription was performed with the Takara RNA PCR Kit (Takara, Japan). The primers used for the amplification of the genomic fragments of PDCoV strain CHN-HN-2014 were those described by Wang et al., with some modifications to allow their hybridization to all reported PDCoV strains (Wang et al., 2014b). The genomic fragments were assembled with DNASTar Lasergene 7.0. A genome homology analysis and phylogenetic analysis were performed with the DNASTar Lasergene 7.0 and MEGA 7.0.14 software (<http://www.megasoftware.net/>), respectively.

### 2.6. Animal experiments

All the pigs used in this study were purchased from a Hubei White pig foundation seed farm. And the pigs were all negative for PDCoV, PEDV, transmissible gastroenteritis coronavirus (TGEV), pseudorabies (PRV), and porcine circovirus 2 (PCV-2) by PCR test. The sows and pigs were also serum virus neutralizing antibody negative for PDCoV. The 5-day-old pigs were randomized into two groups, eight for PDCoV inoculation and four as the negative control; the 21-day-old pigs were also randomized into two groups, five for PDCoV inoculation and five as the negative control (Table 1). All the groups were housed in separate rooms.

After acclimation for 24 h at our research facility, the PDCoV-challenged groups were orally inoculated with the PDCoV isolate at a titer of  $1 \times 10^{8.0} \text{TCID}_{50}/\text{ml}$  (it is equivalent to  $10^9$  viral RNA

**Table 1**  
Experimental design of PDCoV strain CHN-HN-2014 pathogenicity.

Age	Group	n	Inoculation	Pigs ID
5 days	Challenged	8	PDCoV $1 \times 10^{8.0}$ TCID <sub>50</sub> /ml; 10 ml/pig	1 <sup>*</sup> , 2, 3, 4, 5, 6, 7 <sup>*</sup> , 8
	Control	4	Maintenance medium; 10 ml/pig	9 <sup>*</sup> , 10, 11 <sup>*</sup> , 12
21 days	Challenged	5	PDCoV $1 \times 10^{8.0}$ TCID <sub>50</sub> /ml; 10 ml/pig	362, 366, 371, 372, 378
	Control	5	Maintenance medium; 10 ml/pig	363, 365, 368, 369, 379

<sup>\*</sup> Four pigs were necropsied at 4 days post inoculation.

copies/ml; 10 ml per pig), and the control groups were orally inoculated with volume-matched maintenance medium. Clinical symptoms, such as vomiting, diarrhea, lethargy, and appetite loss, were observed daily. Two of the challenged pigs and two of the negative control pigs were selected randomly from the 5-day-old pig group for necropsy at 4 DPI. At necropsy, the lung, liver, kidney, spleen, duodenum, jejunum, ileum, colon, and blood were collected for analysis with real-time RT-PCR. The duodenum, jejunum, and ileum were also analyzed with histopathology and immunohistochemistry.

The piglet body temperatures were recorded before inoculation and then every day until 14 DPI. Fecal swabs were collected before inoculation and then every day until 21 DPI.

### 2.7. Real-time RT-PCR

Each fecal swab was diluted and homogenized in 1 ml of DMEM, and then centrifuged at  $4200 \times g$  at  $4^\circ C$  for 10 min. An aliquot (200  $\mu$ l) of supernatant was collected for viral RNA extraction. Equal quantities (1 g) of tissue samples were homogenized in 1 ml of DMEM, and 200  $\mu$ l of the supernatant was used for RNA extraction. Serum (200  $\mu$ l) was also used for RNA extraction.

RNA extraction and RT were performed as described above in the complete genomic analysis, and the cDNA was used for real-time RT-PCR. The primers used targeted the N gene of PDCoV, as described by Ma et al. (2015). The standard plasmid was constructed by inserting the entire N gene sequence of PDCoV into the pET-30a vector (Novagen, Germany). Real-time RT-PCR was performed on the Applied Biosystem 7500 Fast Real-Time PCR System (Life Technologies, USA) with SYBR Green Real-Time PCR

Master Mix (Life Technologies). The amplification conditions were:  $95^\circ C$  for 10 min, then 40 cycles of  $95^\circ C$  for 15 s,  $60^\circ C$  for 45 s. In each assay, 10-fold dilutions of the standard plasmid (from  $10^{10}$  to  $10^0$ ) and the negative control (distilled water) were included. Each sample was assayed three times. The quantity of PDCoV viral RNA was calculated based on the results for the standard plasmid. The viral RNA copies in the fecal swab and tissue samples were converted to total viral RNA copies per milliliter of homogenized rectal swab supernatant or per gram of tissue, respectively.

### 2.8. Histology and immunohistochemistry

At necropsy, the duodenum, jejunum, and ileum of the 5-day-old pigs from the challenged and control groups were separated and routinely fixed in 10% formalin for 36 h, and then dehydrated, embedded, sectioned, and mounted onto glass slides. After they were stained with hematoxylin and eosin (H&E), the slides were examined and analyzed with conventional microscopy. Sections (5  $\mu$ m) of formalin-fixed paraffin-embedded tissues were placed onto positively charged glass slides and the slides were air dried for 30 min. The tissue sections were deparaffinized, and then rinsed and incubated with target retrieval solution (Sigma-Aldrich, USA). After the sections were blocked, they were incubated with a PDCoV-N-protein-specific monoclonal antibody (diluted 1:1600) as the primary antibody for 30 min at  $37^\circ C$ . They were then incubated with biotinylated goat anti-mouse IgG secondary antibody (Boster, China). The biotin was probed by incubation with the SABC Elite complex (Boster), and the samples were finally visualized with a 3,3'-diaminobenzidine (DAB) chromogen kit (Dako, Denmark). Hematoxylin was used for counterstaining. The

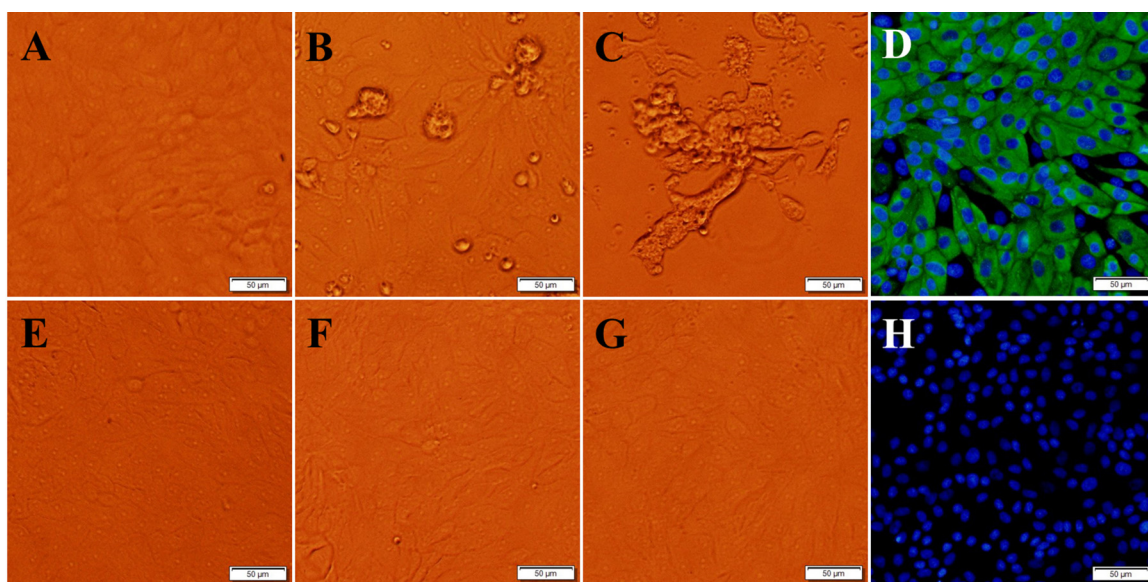


**Fig. 1.** Cytopathic effect and IFA staining of LLC-PK1 cells infected with PDCoV strain CHN-HN-2014. (A, B and C) Cytopathic effect (CPE) in LLC-PK1 cells at 12 h (A), 24 h (B), and 36 h (C) after PDCoV CHN-HN-2014 infection. (E, F and G) Morphology of the control LLC-PK1 cells, without PDCoV infection, at 12 h (E), 24 h (F), and 36 h (G). (D, H) LLC-PK1 cells were infected (D) or mock-infected with PDCoV CHN-HN-2014. At 24 h postinfection, an immunofluorescence assay (IFA) was performed with a monoclonal antibody against PDCoV N protein. Bar, 50  $\mu$ m.

immunohistochemistry slides were evaluated by a veterinary pathologist according to the evaluation system of histology and immunohistochemistry by Jung et al. (2014). Tissues of pigs from the PDCoV-challenged and negative control groups were used as the positive and negative samples, respectively.

### 3. Results

#### 3.1. Viral isolation, plaque purification, and propagation

Twenty-one PDCoV-positive samples were attempted to isolate the virus, but only one PDCoV strain, designated CHN-HN-2014, was successfully isolated from a sample of small intestinal contents collected on a commercial pig farm in Henan Province, China. To our surprise, an obvious CPE was observed 24 h after the first round of inoculation of the intestinal sample containing CHN-HN-2014. This PDCoV isolate was then plaque purified at the second passage, and tested negative for PEDV, TGEV, PRV, PCV-2. A typical CPE, characterized by enlarged, rounded, and clustered cells, was observed at 12 h and 24 h postinfection during the serial

propagation of the virus (Fig. 1A and B). The infected cells showed lysis and detachment from the cell monolayer at 36 h postinfection (Fig. 1C).

The propagation of PDCoV strain CHN-HN-2014 in LLC-PK1 cells was confirmed with IFA staining with a monoclonal antibody directed against the PDCoV N protein. As shown in Fig. 1D, PDCoV-N-protein-specific immunofluorescence was detected in most cells at 24 h postinfection, and the N protein was predominantly located in the cytoplasm.

The particles of PDCoV strain CHN-HN-2014 purified from infected LLC-PK1 cells were also examined with electron microscopy (EM). Typical crown-shaped particles with spiky surface projections were observed with negative staining on EM, and the particles were 80–160 nm in diameter (Fig. 2A and B).

#### 3.2. Characterization of the PDCoV strain CHN-HN-2014 genome

Before the genome of PDCoV strain CHN-HN-2014 was characterized, the complete genome was sequenced and deposited in GenBank under accession number KT336560. The complete

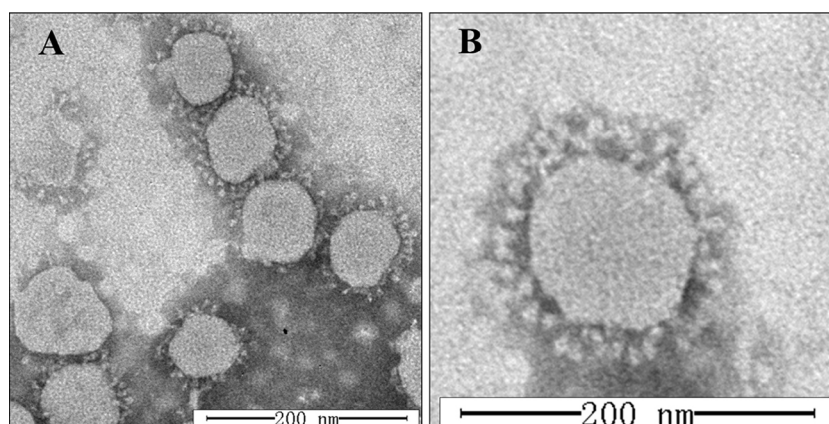


Fig. 2. Electron microscopic images of purified PDCoV particles. (A) Microscopic image of several PDCoV particles. (B) Microscope image of a single PDCoV particle. Bar, 200 nm.

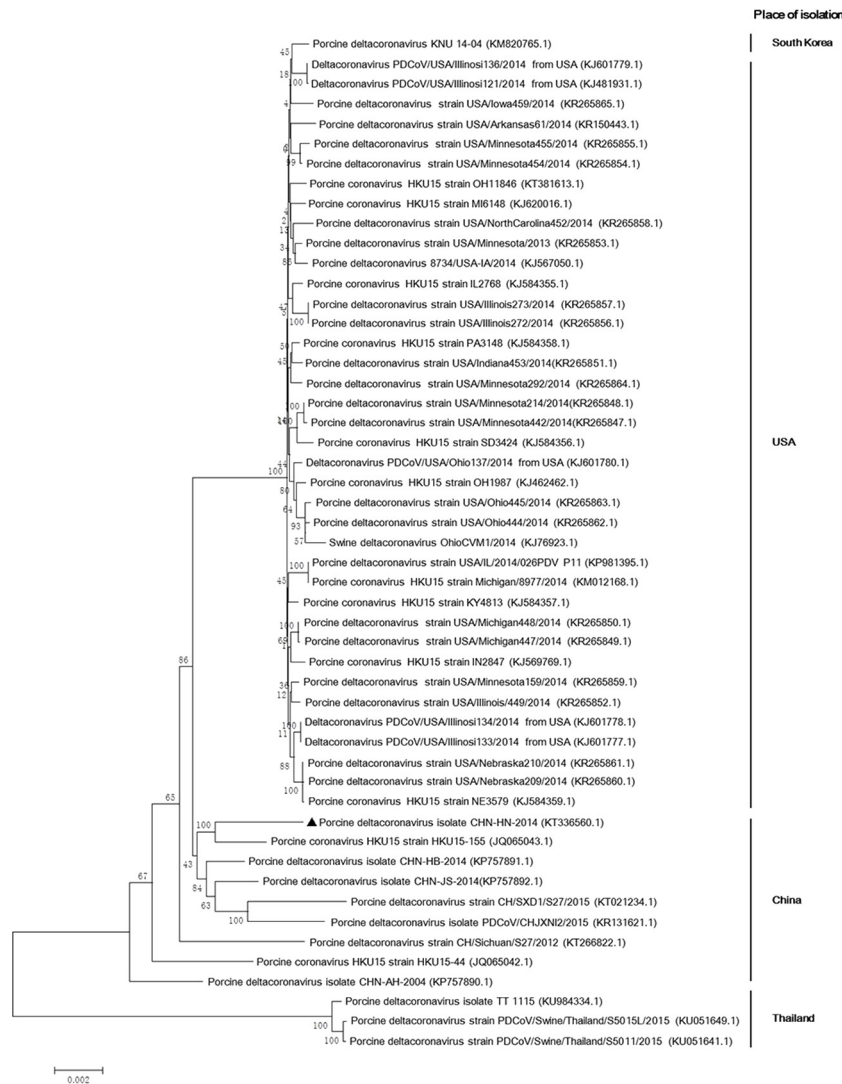
	ORF 1a	ORF 1a	S gene	3' UTR
	1736 1760	2050 2052	19460 19468	25140 25155
	CAGTTTAAAGATCCC	GACCGCTTGGTAAG	GCTAAATAAATTTT	TCTTCCTTAAACCC
	.....	.....	.....	.....
	.....	.....	.....	.....
	.....	.....	.....	.....
<b>China</b>				
Porcine coronavirus HKU15 strain HKU15-44 (JQ065042.1)	.....	.....	.....	.....
Porcine coronavirus HKU15 strain HKU15-155 (JQ065043.1)	.....	.....	.....	.....
Porcine deltacoronavirus isolate CHN-AM-2008 (KF377892.1)	.....	.....	.....	.....
<b>Porcine deltacoronavirus isolate CHN-HN-2014 (KT336560.1)</b>	.....	.....	.....	.....
Porcine deltacoronavirus isolate CHN-78-2014 (KF375782.1)	.....	.....	.....	.....
Porcine deltacoronavirus isolate CHN-48-2014 (KF375781.1)	.....	.....	.....	.....
Porcine deltacoronavirus strain CH/Sichuan/S27/2012 (KT266822.1)	.....	.....	.....	.....
Porcine deltacoronavirus strain CH/SKD1/S27/2015 (KT021234.1)	.....	.....	.....	.....
Porcine deltacoronavirus isolate FDCoV/CHN/J22/2015 (KR131621.1)	.....	.....	.....	.....
Porcine deltacoronavirus strain FDCoV/Swine/Thailand/85011/2015 (KU051641.1)	.....	.....	.....	.....
Porcine deltacoronavirus strain FDCoV/Swine/Thailand/85015L/2015 (KU051649.1)	.....	.....	.....	.....
<b>Thailand</b>				
Porcine deltacoronavirus isolate TT 1115 (KP794334.1)	.....	.....	.....	.....
Porcine deltacoronavirus HKU 14-04 (KM262765.1)	.....	.....	.....	.....
<b>South Korea</b>				
Porcine coronavirus HKU15 strain IL2768 (KJ584355.1)	.....	.....	.....	.....
Porcine deltacoronavirus 8734/USA-IA/2014 (KJ267050.1)	.....	.....	.....	.....
Porcine deltacoronavirus strain USA/Arkansas/61/2014 (KR1550442.1)	.....	.....	.....	.....
Deltacoronavirus PDCoV/USA/Illinois121/2014 from USA (KJ481931.1)	.....	.....	.....	.....
Deltacoronavirus PDCoV/USA/Illinois133/2014 from USA (KJ601777.1)	.....	.....	.....	.....
Deltacoronavirus PDCoV/USA/Illinois134/2014 from USA (KJ601778.1)	.....	.....	.....	.....
Deltacoronavirus PDCoV/USA/Illinois136/2014 from USA (KJ601779.1)	.....	.....	.....	.....
Porcine deltacoronavirus strain USA/Illinois272/2014 (KR265856.1)	.....	.....	.....	.....
Porcine deltacoronavirus strain USA/Illinois273/2014 (KR265857.1)	.....	.....	.....	.....
Porcine deltacoronavirus strain USA/Illinois449/2014 (KR265852.1)	.....	.....	.....	.....
Porcine coronavirus HKU15 strain IN2847 (KJ256976.1)	.....	.....	.....	.....
Porcine deltacoronavirus strain USA/Indiana453/2014 (KR265851.1)	.....	.....	.....	.....
Porcine deltacoronavirus strain USA/Iowa459/2014 (KR265865.1)	.....	.....	.....	.....
Porcine coronavirus HKU15 strain KY4813 (KJ258387.1)	.....	.....	.....	.....
Porcine coronavirus HKU15 strain MI6148 (KJ262016.1)	.....	.....	.....	.....
Porcine coronavirus HKU15 strain Michigan/8977/2014 (KR012168.1)	.....	.....	.....	.....
Porcine deltacoronavirus strain USA/Michigan447/2014 (KR265849.1)	.....	.....	.....	.....
Porcine deltacoronavirus strain USA/Michigan448/2014 (KR265850.1)	.....	.....	.....	.....
<b>USA</b>				
Porcine deltacoronavirus strain USA/Minnesota/2013 (KR265853.1)	.....	.....	.....	.....
Porcine deltacoronavirus strain USA/Minnesota139/2014 (KR265859.1)	.....	.....	.....	.....
Porcine deltacoronavirus strain USA/Minnesota214/2014 (KR265848.1)	.....	.....	.....	.....
Porcine deltacoronavirus strain USA/Minnesota292/2014 (KR265864.1)	.....	.....	.....	.....
Porcine deltacoronavirus strain USA/Minnesota442/2014 (KR265847.1)	.....	.....	.....	.....
Porcine deltacoronavirus strain USA/Minnesota454/2014 (KR265854.1)	.....	.....	.....	.....
Porcine deltacoronavirus strain USA/Minnesota455/2014 (KR265855.1)	.....	.....	.....	.....
Porcine coronavirus HKU15 strain NB3579 (KJ258435.1)	.....	.....	.....	.....
Porcine deltacoronavirus strain USA/Nebraska6209/2014 (KR265860.1)	.....	.....	.....	.....
Porcine deltacoronavirus strain USA/Nebraska210/2014 (KR265861.1)	.....	.....	.....	.....
Porcine deltacoronavirus strain USA/NorthCarolina452/2014 (KR265858.1)	.....	.....	.....	.....
Porcine coronavirus HKU15 strain OH1897 (KJ264462.1)	.....	.....	.....	.....
Porcine deltacoronavirus strain USA/Ohio144/2014 (KR265862.1)	.....	.....	.....	.....
Porcine deltacoronavirus strain USA/Ohio145/2014 (KR265863.1)	.....	.....	.....	.....
Swine deltacoronavirus OhioCMI/2014 (KJ76923.1)	.....	.....	.....	.....
Porcine coronavirus HKU15 strain PA3148 (KJ258436.1)	.....	.....	.....	.....
Porcine coronavirus HKU15 strain SD2424 (KJ264356.1)	.....	.....	.....	.....
Porcine deltacoronavirus strain USA/IL/2014/0249DF P11 (KP981395.1)	.....	.....	.....	.....

Fig. 3. Four main deletions or insertions in the complete genome alignment. A multiple sequence alignment was constructed with ClustalW in the DNASTar software. PDCoV strain CHN-HN-2014 is indicated in bold and highlighted with a box. A dash indicates that the nucleotide exactly matches the consensus sequence. A dot indicates that the nucleotide is deleted relative to the reference sequence.

genome shared 91.6%–99.4% nucleotide identity with the other 50 PDCoV strains available in GenBank. Compared with those PDCoV strains, a 3-nt deletion was observed in the S gene of PDCoV strain CHN-HN-2014, which was also present in most Chinese PDCoV strains, except PDCoV strains HKU15-44 and CHN-AH-2004. Compared with PDCoV strains CHN-AH-2004 and HKU15-155, a 3-nt insertion was present in the 3' untranslated region (UTR), as in most of the PDCoV strains. However, three Thailand PDCoV strains contained a 6-nt insertion and a 9-nt insertion in open reading frame (ORF) 1a and a cytosine deletion in the 3' UTR (Fig. 3). A phylogenetic analysis demonstrated that the PDCoV strains from the United States and South Korea clustered into a large clade, whereas PDCoV strain CHN-HN-2014 clustered with other PDCoV strains detected in China since 2014, and suggests that the US and South Korean clade and the Chinese clade might share a common evolutionary ancestor (Fig. 4). Interestingly, the PDCoV strains from Thailand clustered in a clade quite distinct (Fig. 4).

### 3.3. Clinical manifestations of pigs challenged with PDCoV CHN-HN-2014

To evaluate the pathogenicity of PDCoV strain CHN-HN-2014, 5-day-old and 21-day-old pigs were challenged with the same dose of the virus. All the pigs from the control groups were active and fleshy during the study. However, in the 5-day-old challenged pig group, 4/8 pigs showed mild diarrhea at 1 DPI, and more pigs had developed diarrhea, together with lethargy, vomiting, and anorexia, at 2–6 DPI (Fig. 5A and B). The progression of diarrhea was most severe at 4–6 DPI and the pigs gradually recovered thereafter (Table 2). In the 21-day-old challenged pig group, 1/5 pigs had mild diarrhea accompanied by anorexia at 1 DPI, and 4/5 pigs developed mild or watery diarrhea at 4 DPI (Fig. 5C). The pigs had completely recovered at 7–8 DPI (Table 3). Despite the watery diarrhea accompanied by vomiting, lethargy, and anorexia, no mortality occurred during the study. The body temperatures of all the pigs were recorded at 0–14 DPI, but there were no significant differences between the challenged and control pigs ( $P > 0.05$ ).



**Fig. 4.** Phylogenetic analysis of the complete genomic nucleotide sequences of 51 PDCoV strains available in GenBank. Complete PDCoV genomes are indicated by strain names and GenBank accession numbers. The names of country in the right of the phylogenetic tree indicate the places of PDCoV strains. PDCoV strain CHN-HN-2014 is indicated with a triangle. The phylogenetic tree was constructed with the neighbor-joining method in the MEGA 7.0.14 software (<http://www.megasoftware.net>). A bootstrap analysis was performed with 1000 replicates and the bootstrap values are indicated on each branch. Scale bar indicates nucleotide substitutions per site.



**Fig. 5.** Clinical assessment of piglets challenged with PDCoV strain CHN-HN-2014. (A, D) Five-day-old piglets at 4 days postinoculation (DPI) with PDCoV strain CHN-HN-2014 (A) or DMEM medium (D). (C, D) Representative images of 5-day-old piglets (C) and 21-day-old piglets (D) with diarrhea at 4 DPI with PDCoV strain CHN-HN-2014. (E, F) Representative images of 5-day-old piglets (E) and 21-day-old piglets (F) at 4 DPI after treatment with DMEM.

**Table 2**  
Clinical observation records of 5-day-old piglets challenged with PDCoV strain CHN-HN-2014.

DPI	Clinical observation	Fecal consistency		
		Normal	Mild diarrhea	Watery diarrhea
0	All active and eating well	8/8	0/8	0/8
1	All active; 25% vomiting and anorexia	4/8	4/8	0/8
2	25% lethargy, vomiting and anorexia	2/8	4/8	2/8
3	75% lethargy, vomiting and anorexia	1/8	4/8	3/8
4*	All lethargy; 83% vomiting and anorexia	0/6	2/6	4/6
5	All lethargy; 83% vomiting and anorexia	0/6	2/6	4/6
6	All lethargy; 83% vomiting and anorexia	2/6	2/6	2/6
7	50% lethargy and anorexia	4/6	2/6	0/6
8	All active and eating well	6/6	0/6	0/6
9–21	All active and eating well	6/6	0/6	0/6

\* Two pigs were necropsied at 4 days post inoculation.

**Table 3**  
Clinical observation records of 21-day-old piglets challenged with PDCoV strain CHN-HN-2014.

DPI	Clinical observation	Fecal consistency		
		Normal	Mild diarrhea	Watery diarrhea
0	All active and eating well	5/5	0/5	0/5
1	All active; 20% anorexia	4/5	1/5	0/5
2	All lethargy, and anorexia	2/5	2/5	1/5
3	20% lethargy, anorexia	2/5	1/5	2/5
4	40% lethargy, anorexia	1/5	2/5	2/5
5	20% lethargy, anorexia	1/5	3/5	1/5
6	20% lethargy, anorexia	3/5	2/5	0/5
7	All active and eating well	5/5	0/5	0/5
8	All active and eating well	5/5	0/5	0/5
9–21	All active and eating well	5/5	0/5	0/5

### 3.4. Fecal shedding and virus distribution

We also determined the fecal viral shedding and virus distribution in the PDCoV-challenged pigs. PDCoV RNA was detected in 5/8 and 3/5 rectal swab samples from the 5-day-old and 21-day-old pigs, respectively, at 1 DPI, and more fecal samples were positive thereafter. PDCoV RNA copies reached a peak of  $10^6$ – $10^8$  copies per milliliter of homogenized rectal swab supernatant at 2–7 DPI, and PDCoV RNA was detected until 14 DPI and 18 DPI in the 5-day-old and 21-day-old pigs, respectively (Fig. 6A and B). No PDCoV RNA was detected in the negative control pigs during the study.

The distribution of the PDCoV virus in different tissues was also tested in two 5-day-old piglets at necropsy at 4 DPI. Viral RNA was detected in 2/2 duodenums (average  $10^{7.01}$  copies/g), 2/2 jejunums (average  $10^{8.60}$  copies/g), 1/2 ileums ( $10^{8.49}$  copies/g), and 2/2 colons (average  $10^{8.97}$  copies/g). It was also detected in 1/2 spleens ( $10^{6.39}$  copies/g), 1/2 kidneys ( $10^{7.23}$  copies/g), and 1/2 lungs ( $10^{5.29}$  copies/g), but no viral RNA was detected in the liver or blood.

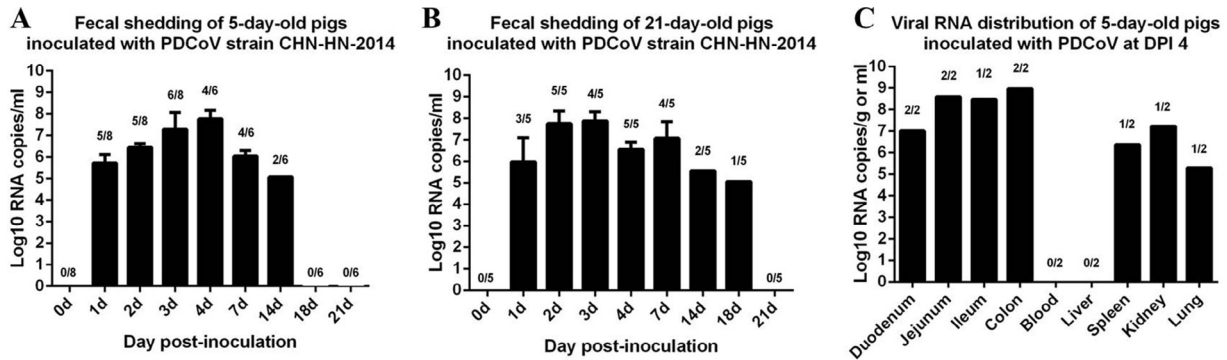


**Fig. 6.** Fecal viral shedding and virus distribution in PDCoV-challenged pigs. (A) Fecal viral shedding in 5-day-old pigs challenged with PDCoV strain CHN-HN-2014. (B) Fecal viral shedding in 21-day-old pigs challenged with PDCoV strain CHN-HN-2014. (C) Virus distribution at 4 DPI in 5-day-old pigs challenged with PDCoV.

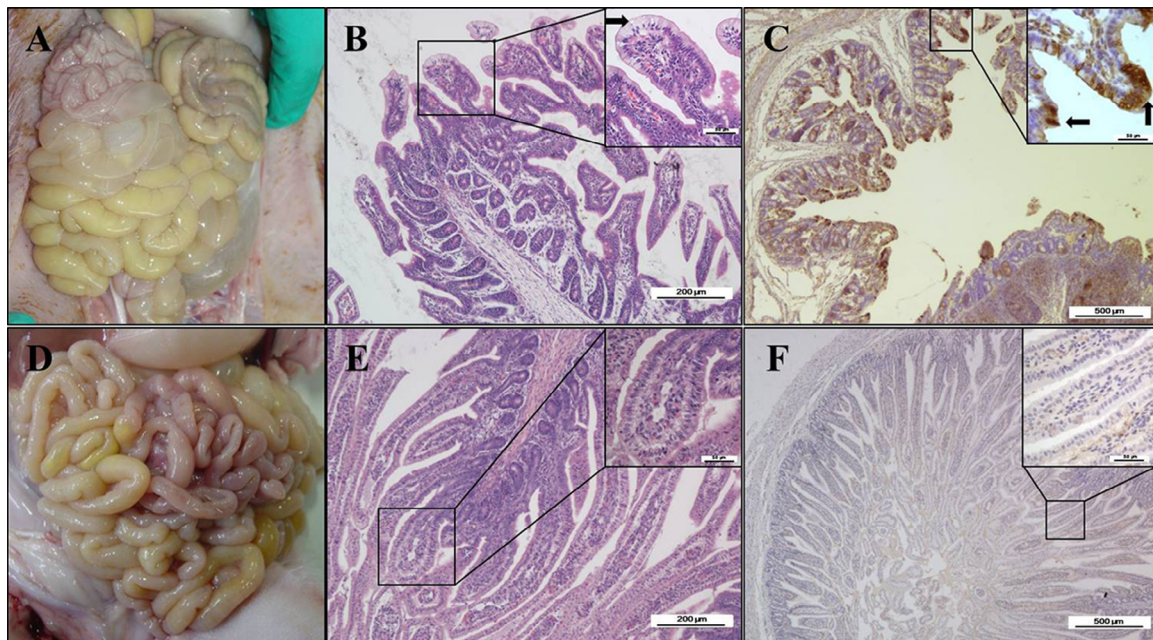


**Fig. 7.** Intestinal lesions of PDCoV-challenged pig at 4 DPI. (A) Macroscopic lesions of a PDCoV-challenged pig at 4 DPI. (B) H&E-stained jejunum tissue section of a PDCoV-challenged pig. (C) Immunohistochemically stained jejunum tissue section of a PDCoV-challenged pig. (D) Macroscopic picture of a control pig at 4 DPI. (E) H&E-stained jejunum tissue section of a control pig. (F) Immunohistochemically stained jejunum tissue section of a control pig. The arrow in (B) indicates the typical histological lesions of swelling and vacuolation of the superficial villous, and the arrows in (C) indicate the immunohistochemical staining of PDCoV antigen in epithelial cells. Scale bars are shown in each picture.

(Fig. 6C). No PDCoV RNA was detected in the tissue samples from the control pigs.

### 3.5. Gross pathology, histopathology, and immunohistochemistry

Pathology tests were also conducted on the PDCoV challenged pigs. The small intestines were clearly transparent, thin-walled, and gas-distended, and yellow watery contents had accumulated in them in the PDCoV-challenged pigs by necropsy at 4 DPI (Fig. 7A). No lesions were observed in any other organs of the PDCoV-challenged pigs or in the organs in the negative control pigs at necropsy (Fig. 7D). Mild intestinal lesions consistent with viral enteritis were observed in the PDCoV-challenged pigs at necropsy at 4 DPI. Lesions were apparent in the distal jejunum and ileum but were not observed in the duodenum. The villous atrophy was apparent in the small intestines, especially in the jejunum and ileum (Table 4). The typical histological lesions were characterized by swelling and vacuolation of the superficial villous epithelial

cells, and small numbers of lymphocytes and neutrophils had infiltrated the intestinal lamina propria (Fig. 7B).

Consistent with the histopathological results, the immunohistochemical analysis detected PDCoV antigen in the cytoplasm of

**Table 4**

Histology and immunohistochemistry analysis of intestinal infected with PDCoV strain CHN-HN-2014.

Group	Pig ID	VH: CD, mean ( $\pm$ SD) <sup>a</sup>	Antigen detection in the intestinal <sup>b</sup>		
			Duodenum	Jejunum	Ileum
challenged	1	2.9 (0.6)	+	+++	++
	8	3.8 (1.1)	+	+++	++
control	9	6.1 (0.7)	-	-	-
	11	5.6 (0.3)	-	-	-

<sup>a</sup> VH: CD, ratio of villous height to crypt depth.

<sup>b</sup> Antigen detection by immunohistochemical staining: +, 1%–30% of epithelial cells showed staining; ++, 31%–60% of epithelial cells showed staining; +++, 61%–100% of epithelial cells showed staining; -, no epithelial cells showed staining.

the villous enterocytes of the PDCoV-challenged pigs (Fig. 7C). PDCoV immunohistochemical staining was positive in the duodenums, jejunums, and ileums of both the PDCoV-challenged pigs at necropsy at 4 DPI but was negative in the corresponding tissues of the negative control pigs (Table 4).

#### 4. Discussion

Since the first detection of PDCoV in pigs with diarrhea in 2014 in the United States and the first confirmation of its pathogenicity in pigs (Wang et al., 2014a; Jung et al., 2014), this novel swine enteric coronavirus has drawn wide attention in different countries. In China, several groups have investigated the prevalence of PDCoV in different provinces. A survey conducted by Song et al. demonstrated a prevalence of 33.71%, and a survey by Chen et al. showed a prevalence of 23.4% in different areas of China (Chen et al., 2015a, 2015b; Song et al., 2015). Although the prevalence of PDCoV in China is confirmed, the characteristics of the Chinese PDCoV had not been determined.

To isolate cell-culture-adapted PDCoV strains, 21 positive samples (five intestinal contents and 16 feces) were used to isolate PDCoV in LLC-PK1 cells in this study. However, only PDCoV strain CHN-HN-2014 was successfully isolated and confirmed with typical CPE, IFA, and EM. This PDCoV isolate caused obvious CPE on LLC-PK1 cells 24 h after their inoculation with the PDCoV-positive intestinal sample. After plaque purification and several passages, the viral titer was  $10^{8.0}$  TCID<sub>50</sub>/ml, suggesting that this PDCoV isolate was highly adapted to LLC-PK1 cells. Among the samples from which we attempted to isolate the virus, 12 of the feces samples and two of the intestinal contents samples showed cell toxicity. The success rate (1/21) of PDCoV isolation in this study was quite low. In previous studies, most of the PEDV strains have been isolated from intestinal contents samples (Chen et al., 2014; Oka et al., 2014), and this was also reported by Hu et al., in their attempts to isolate PDCoV from different samples (Hu et al., 2015). Based on these results, we speculate that intestinal contents are ideal sources for PEDV and PDCoV, or even other enteric swine CoVs isolation. This might be attributable to the relatively low rate of cytotoxicity in intestinal contents samples, but many other factors, including the titer of the infectious virus in the samples and the sample preservation conditions, might also contribute to successful PDCoV isolation.

According to a multiple sequence alignment and phylogenetic analysis, all the known PDCoV strains share high nucleotide identities. However, the PDCoV strain CHN-HN-2014 genome is more similar to those of strains from China, the United States, and South Korea than to Thai strains. Previous studies have shown that the determinants of coronavirus tropism are located at the S1 region of the S protein (Masters, 2006), and that the S protein of the CoVs might be strongly associated with the pathogenicity and virulence of the virus. One of the largest variations in the PDCoV S gene detected to date is a 3-nt deletion in the S1 region (Dong et al., 2015; Wang et al., 2015a, 2015b; Janetanakit et al., 2016). A 3-nt deletion in the S gene relative to the S genes of the US and South Korean strains, which causes the deletion of an amino acid in the S protein, was also observed in PDCoV strain CHN-HN-2014. Given that PDCoV strain CHN-HN-2014 is pathogenic, like the US strains, this 3-nt deletion alone might not determine the pathogenicity of PDCoV. However, the recently emerging PDCoV strains in Thailand are highly virulent, causing a mortality rate of 19.22% on pig farms (Janetanakit et al., 2016). In our phylogenetic analysis, the PDCoV strains from Thailand clearly clustered in a separate clade (Fig. 4), and in the genomic sequence alignment, they showed several distinct variations in ORF 1a and the 3' UTR compared with the other strains (Fig. 3). This implies that these unique variations contribute to the strong virulence of the Thai strains.

The pathogenicity of PDCoV strains OH-FD22 and OH-FD100 was first confirmed in 11–14 day-old gnotobiotic pigs (Jung et al., 2015). The pathogenicity of a PDCoV cell-culture-adapted strain, USA/IL/2014, was subsequently confirmed in 5-day-old conventional pigs (Chen et al., 2015a, 2015b). The pathogenicity of another cell-culture-adapted strain, PdcV CVM1, was later tested in 10-day-old gnotobiotic and conventional pigs, and the PDCoV Ohio CVM strain (from intestinal contents) was tested in 19-day-old gnotobiotic pigs (Ma et al., 2015). Consequently, it has been confirmed that PDCoV is enteropathogenic in pigs of different age, from 5 to 19 days old. In the present study, 5-day-old and 21-day-old pigs were challenged with the same dose of PDCoV strain CHN-HN-2014, and the severity of their clinical symptoms was compared under the same conditions. Our clinical observations show that the 5-day-old pigs were more susceptible to PDCoV infection than the 21-day-old pigs. This age-dependent disease severity in PDCoV infection is consistent with previous reports of PEDV and TGEV infections (Moon et al., 1975; Shibata et al., 2000) and might be attributable to the lower turnover rate of enterocytes in 5-day-old pigs than in 21-day-old pigs during PDCoV infection, as has been described in PEDV infection (Jung and Saif, 2015). A recent report showed that an outbreak of PDCoV infection was observed in gilts and sows in Thailand (Janetanakit et al., 2016), indicating that the pathogenicity of PDCoV is not confined to piglets.

The viral fecal shedding pattern in the PDCoV-challenged pigs was detected with real-time RT-PCR. The PDCoV viral RNA shedding patterns reported in previous studies were limited to 7 DPI. In this study, we extended the observation period to 21 DPI. Surprisingly, viral shedding was detected in one of the 21-day-old challenged pigs at 18 DPI, but had ceased at 14 DPI in the 5-day-old pigs. Considering the differences in the clinical symptoms and disease severity of the 5- and 21-day-old pigs, we speculate that this abnormal result might be caused by individual differences in the pigs. In previous studies of PEDV-challenged pigs, viral RNA was detected beyond 21 DPI (Madson et al., 2014; Lin et al., 2015), which might indicate that the virulence of PDCoV is milder than that of PEDV in pigs. The viral RNA distribution in the 5-day-old PDCoV-challenged pigs was also tested. The intestines contained relatively high levels of viral RNA copies compared with the other tissues, and we detected no PDCoV viral RNA in the blood. Previous studies are inconsistent about virus detection in the blood (Chen et al., 2015a, 2015b; Jung et al., 2015; Ma et al., 2015), and these differences might arise from the different time points at which the blood was sampled or the diversity among the different PDCoV strains. Mild interstitial pneumonia has also been identified in the lungs of PDCoV-infected pigs (Ma et al., 2015). In this study, viral RNA was also detected in 1/2 lungs, 1/2 spleens, and 1/2 kidneys, but no gross lesions were observed in these tissues. Obvious gross lesions were only observed in the small intestines of the 5-day-old pigs at necropsy at 4 DPI. A previous study revealed that SARS-CoV infected a wide range of organs, although the respiratory tract was the major target of infection (Gu and Korteweg, 2007). PDCoV infection might also infect multiple organs in pigs, but the major target organ is the intestinal tract. In previous reports, microscopic lesions associated with PEDV infection were observed in all sections of the small intestine (Madson et al., 2014), but microscopic lesions were only observed in the jejunum and ileum in this study, indicating that PDCoV infection is less severe in the intestinal tract than PEDV infection. All these data confirm that PDCoV strain CHN-HN-2014 induces enteric infections in pigs.

#### 5. Conclusion

PDCoV strain CHN-HN-2014, which was associated with diarrhea in pigs in Henan Province, China, was successfully



isolated in the LLC-PK1 cell line. To our knowledge, this is the first characterization of a PDCoV isolate in China. Animal experiments confirmed that this PDCoV isolate is enteropathogenic and causes severe intestinal disease in 5-day-old and 21-day-old pigs. It also displays age-dependent disease severity in pigs of different age, as do PEDV and TGEV. Therefore, efficient diagnostic assays and vaccines for this newly emerging PDCoV are urgently required.

## Acknowledgements

This work was supported by the National Key R&D Plan of China (2016YFD0500103), the Key Technology R&D Programme of China (2015BAD12B02), and the Natural Science Foundation of Hubei Province (2014CFA009).

## References

- Chen, Q., Li, G., Stasko, J., Thomas, J.T., Stensland, W.R., Pillatzki, A.E., Gauger, P.C., Schwartz, K.J., Madson, D., Yoon, K.J., Stevenson, G.W., Burrough, E.R., Harmon, K.M., Main, R.G., Zhang, J., 2014. Isolation and characterization of porcine epidemic diarrhea viruses associated with the 2013 disease outbreak among swine in the United States. *J. Clin. Microbiol.* 52, 234–243.
- Chen, F., Zhu, Y., Wu, M., Ku, X., Yao, L., He, Q., 2015a. Full-length genome characterization of chinese porcine deltacoronavirus strain CH/SXD1/2015. *Genome Announc.* 3, e01284–15.
- Chen, Q., Gauger, P., Stafne, M., Thomas, J., Arruda, P., Burrough, E., Madson, D., Brodie, J., Magstadt, D., Derscheid, R., Welch, M., Zhang, J., 2015b. Pathogenicity and pathogenesis of a United States porcine deltacoronavirus cell culture isolate in 5-day-old neonatal piglets. *Virology* 482, 51–59.
- Dong, N., Fang, L., Zeng, S., Sun, Q., Chen, H., Xiao, S., 2015. Porcine deltacoronavirus in mainland China. *Emerg. Infect. Dis.* 21, 2254–2255.
- Gu, J., Korteweg, C., 2007. Pathology and pathogenesis of severe acute respiratory syndrome. *Am. J. Pathol.* 170, 1136–1147.
- Homwong, N., Jarvis, M.C., Lam, H.C., Diaz, A., Rovira, A., Nelson, M., Marthaler, D., 2016. Characterization and evolution of porcine deltacoronavirus in the United States. *Prev. Vet. Med.* 123, 168–174.
- Hu, H., Jung, K., Vlasova, A.N., Chepngeno, J., Lu, Z., Wang, Q., Saif, L.J., 2015. Isolation and characterization of porcine deltacoronavirus from pigs with diarrhea in the United States. *J. Clin. Microbiol.* 53, 1537–1548.
- Janetanakit, T., Lumyai, M., Bunpapong, N., Boonyapisitsopa, S., Chaiyawong, S., Nonthabenjawan, N., Kesdaengsakonwut, S., Amonsin, A., 2016. Porcine deltacoronavirus, Thailand, 2015. *Emerg. Infect. Dis.* 22, 757–759.
- Jung, K., Saif, L.J., 2015. Porcine epidemic diarrhea virus infection Etiology, epidemiology, pathogenesis and immunoprophylaxis. *Vet. J.* 204, 134–143.
- Jung, K., Wang, Q., Scheuer, K.A., Lu, Z., Zhang, Y., Saif, L.J., 2014. Pathology of US porcine epidemic diarrhea virus strain PC21A in gnotobiotic pigs. *Emerg. Infect. Dis.* 20, 662–665.
- Jung, K., Hu, H., Eyerly, B., Lu, Z., Chepngeno, J., Saif, L.J., 2015. Pathogenicity of 2 porcine deltacoronavirus strains in gnotobiotic pigs. *Emerg. Infect. Dis.* 21, 650–654.
- Jung, K., Hu, H., Saif, L.J., 2016. Porcine deltacoronavirus infection: etiology, cell culture for virus isolation and propagation, molecular epidemiology and pathogenesis. *Virus Res.* doi:http://dx.doi.org/10.1016/j.virusres.2016.04.009.
- Lee, S., Kim, Y., Lee, C., 2015. Isolation and characterization of a Korean porcine epidemic diarrhea virus strain KNU-141112. *Virus Res.* 208, 215–224.
- Lee, J.H., Chung, H.C., Nguyen, V.G., Moon, H.J., Kim, H.K., Park, S.J., Lee, C.H., Lee, G.E., Park, B.K., 2016. Detection and phylogenetic analysis of porcine deltacoronavirus in Korean swine farms, 2015. *Transbound. Emerg. Dis.* 63, 248–252.
- Lin, C.M., Annamalai, T., Liu, X., Gao, X., Lu, Z., El-Tholoth, M., Hu, H., Saif, L.J., Wang, Q., 2015. Experimental infection of a US spike-insertion deletion porcine epidemic diarrhea virus in conventional nursing piglets and cross-protection to the original US PEDV infection. *Vet. Res.* 46, 134.
- Ma, Y., Zhang, Y., Liang, X., Lou, F., Oglesbee, M., Krakowka, S., Li, J., 2015. Origin, evolution, and virulence of porcine deltacoronaviruses in the United States. *MBio* 6 (e00064–15).
- Madson, D.M., Magstadt, D.R., Arruda, P.H., Hoang, H., Sun, D., Bower, L.P., Bhandari, M., Burrough, E.R., Gauger, P.C., Pillatzki, A.E., Stevenson, G.W., Wilberts, B.L., Brodie, J., Harmon, K.M., Wang, C., Main, R.G., Zhang, J., Yoon, K.J., 2014. Pathogenesis of porcine epidemic diarrhea virus isolate (US/Iowa/18984/2013) in 3-week-old weaned pigs. *Vet. Microbiol.* 174, 60–68.
- Marthaler, D., Raymond, L., Jiang, Y., Collins, J., Rossow, K., Rovira, A., 2014. Rapid detection, complete genome sequencing, and phylogenetic analysis of porcine deltacoronavirus. *Emerg. Infect. Dis.* 20, 1347–1350.
- Masters, P.S., 2006. The molecular biology of coronaviruses. *Adv. Virus Res.* 66, 193–292.
- McCluskey, B.J., Haley, C., Rovira, A., Main, R., Zhang, Y., Barder, S., 2015. Retrospective testing and case series study of porcine delta coronavirus in US swine herds. *Prev. Vet. Med.* 123, 185–191.
- Moon, H.W., Kemeny, L.J., Lambert, G., Stark, S.L., Booth, G.D., 1975. Age-dependent resistance to transmissible gastroenteritis of swine: III. Effects of epithelial cell kinetics on coronavirus production and on atrophy of intestinal villi. *Vet. Pathol.* 12, 434–445.
- Oka, T., Saif, L.J., Marthaler, D., Esseili, M.A., Meulia, T., Lin, C.M., Vlasova, A.N., Jung, K., Zhang, Y., Wang, Q., 2014. Cell culture isolation and sequence analysis of genetically diverse US porcine epidemic diarrhea virus strains including a novel strain with a large deletion in the spike gene. *Vet. Microbiol.* 173, 258–269.
- Shibata, I., Tsuda, T., Mori, M., Ono, M., Sueyoshi, M., Uruno, K., 2000. Isolation of porcine epidemic diarrhea virus in porcine cell cultures and experimental infection of pigs of different ages. *Vet. Microbiol.* 72, 173–182.
- Song, D., Zhou, X., Peng, Q., Chen, Y., Zhang, F., Huang, T., Zhang, T., Li, A., Huang, D., Wu, Q., He, H., Tang, Y., 2015. Newly emerged porcine deltacoronavirus associated with diarrhoea in swine in China: identification, prevalence and full-length genome sequence analysis. *Transbound. Emerg. Dis.* 62, 575–580.
- Su, M., Li, C., Guo, D., Wei, S., Wang, X., Geng, Y., Yao, S., Gao, J., Wang, E., Zhao, X., Wang, Z., Wang, J., Wu, R., Feng, L., Sun, D., 2015. A recombinant nucleocapsid protein-based indirect enzyme-linked immunosorbent assay to detect antibodies against porcine deltacoronavirus. *J. Vet. Med. Sci.* 78, 601–606.
- Thachil, A., Gerber, P.F., Xiao, C.T., Huang, Y.W., Opriessnig, T., 2015. Development and application of an ELISA for the detection of porcine deltacoronavirus IgG antibodies. *PLoS One* 10, e0124363.
- Wang, L., Byrum, B., Zhang, Y., 2014a. Detection and genetic characterization of deltacoronavirus in pigs Ohio, USA, 2014. *Emerg. Infect. Dis.* 20, 1227–1230.
- Wang, L., Byrum, B., Zhang, Y., 2014b. Porcine coronavirus HKU15 detected in 9 US states, 2014. *Emerg. Infect. Dis.* 20, 1594–1595.
- Wang, L., Hayes, J., Sarver, C., Byrum, B., Zhang, Y., 2015a. Porcine deltacoronavirus: histological lesions and genetic characterization. *Arch. Virol.* 161, 171–175.
- Wang, Y.W., Yue, H., Fang, W., Huang, Y.W., 2015b. Complete genome sequence of porcine deltacoronavirus strain CH/Sichuan/S27/2012 from mainland China. *Genome Announc.* 3, e00945–15.
- Woo, P.C., Huang, Y., Lau, S.K., Yuen, K.Y., 2010. Coronavirus genomics and bioinformatics analysis. *Viruses* 2, 1804–1820.
- Woo, P.C., Lau, S.K., Lam, C.S., Lau, C.C., Tsang, A.K., Lau, J.H., Bai, R., Teng, J.L., Tsang, C. C., Wang, M., Zheng, B.J., Chan, K.H., Yuen, K.Y., 2012. Discovery of seven novel mammalian and avian coronaviruses in the genus deltacoronavirus supports bat coronaviruses as the gene source of alphacoronavirus and betacoronavirus and avian coronaviruses as the gene source of gammacoronavirus and deltacoronavirus. *J. Virol.* 86, 3995–4008.
- Zhang, X., Hao, J., Zhen, J., Yin, L., Li, Q., Xue, C., Cao, Y., 2015. Rapid quantitation of porcine epidemic diarrhea virus (PEDV) by Virus Counter. *J. Virol. Methods* 223, 1–4.
- Zhang, J., Tsai, Y.L., Lee, P.Y.A., Chen, Q., Zhang, Y., Chiang, C.J., Shen, Y.H., Li, F.C., Chang, H.F.G., Gauger, P.C., Harmon, K.M., Wang, H.T.T., 2016. Evaluation of two singleplex reverse transcription-insulated isothermal PCR tests and a duplex real-time RT-PCR test for the detection of porcine epidemic diarrhea virus and porcine deltacoronavirus. *J. Virol. Methods* 234, 34–42.
- Zhang, J., 2016. Porcine deltacoronavirus: overview of infection dynamics, diagnostic methods, prevalence and genetic evolution. *Virus Res.* doi:http://dx.doi.org/10.1016/j.virusres.2016.05.028.